# INSTRUMENTATION AND DOSIMETRY AT ACCELERATOR FACILITIES

T. Nakamura[1], T. Kurosawa[1], E. Kim[1], M. Takada[1], A. Konno[1],
Y. Uwamino[2], M. Imamura[3], N. Nakao[3], T. Shibata[3], S. Shibata[3], N. Nakanishi[2],
N. Tsujimura[4], T. Yamano[5], H. Ohguchi[6], M. Baba[7], T. Iwasaki[7], S. Matsuyama[7],
H. Nakashima[8], Shun. Tanaka[8], S. Meigo[8], Y. Sakamoto[8], Y. Nakane[8], and Su. Tanaka[9]

[1]Cyclotron and Radioisotope Center, Tohoku University, Aoba, Aramaki, Sendai 980-77, Japan
[2]Institute of Physical and Chemical Research, Hirosawa 2-1, Wako 351-01, Japan
[3]Institute for Nuclear Study, University of Tokyo, Midori-cho 3-2-1, Tanashi 188, Japan
[4]Tokai Works, Power Reactor and Nuclear Fuel Development Corporation, Tokai 319-11, Japan
[5]Tokyo Factory, Fuji Electric Co. Ltd., Fuji-cho, Hino 191, Japan
[6]O-arai Laboratory, Chiyoda Safety Suppliance Co. Ltd., Narita-cho, O-arai 311-13, Japan
[7]Department of Nuclear Engineering, Tohoku University, Aoba, Aramaki, Sendai 980-77, Japan
[8]Tokai Establishment, Japan Atomic Energy Research Institute, Tokai 319-11, Japan
[9]Takasaki Establishment, Japan Atomic Energy Research Institute, Watanuki, Takasaki 370-12, Japan

## INTRODUCTION

The increasing use of high energy and intense particle accelerators has brought the importance of detection and monitoring of high energy neutrons which are most penetrating. The spectrometry and dosimetry of high energy neutrons at accelerator facilities are however very difficult and many works have ever been done, but no established instrumentation still exists.

We have newly developed two types of high energy neutron spectrometers, Bi spallation detector and organic liquid scintillation detector with plastic veto counter, and also two types of wide-energy range personal neutron dosimeters, real-time Si semiconductor detector and CR39 track detector.

The 12.5-cm diam by 12.5-cm long organic liquid scintillation detector, such as NE-213 and BC-501A, was used to measure neutron spectra in the energy range from about 1 MeV up to about 130 MeV, by coupling with the n-$\gamma$ discrimination technique. The thin (5 mm thick) plastic scintillator (NE-102A) was set in front of the neutron detector as a veto counter to discriminate the incoming charged particles. The Bi spallation detector utilizes the Bi(n,xn) reactions up to Bi(n,14n), which have different threshold energies. This detector is very small and light, and can give the gross neutron spectrum over the energy range beyond 100 MeV.

A real time personal dosimeter consists of three types of Si detectors, thermal neutron sensor, fast neutron sensor and gamma-ray sensor (1,2). The thermal neutron sensor which is B-10 doped n-type silicon with a polyethylene radiator detects alpha particles from $^{10}B(n,\alpha)$ and protons from H(n,n) reactions, which is mainly sensitive to neutrons from thermal to 1 MeV. The fast neutron sensor which is p-type silicon with polyethylene is sensitive above 1 MeV, and the gamma-ray sensor is the same as the fast neutron sensor without polyethylene. By taking the weighted sum of two neutron sensor counts, this dosimeter can give the neutron dose equivalent within about 50% errors in wide energy range from thermal to several tens MeV.

A passive personal neutron dosimeter using CR39 was also developed (3). The dosimeter has two pieces of CR39 which are contacted with boron nitride and polyethylene radiators. The former is sensitive to lower energy neutrons and the latter to higher energy neutrons. The weighted sum of two CR39 etch-pits gives neutron dose equivalent within about 30% errors in the energy range from thermal to 15 MeV.

The response functions of these four detectors as a function of neutron energy were measured using the monoenergetic neutron field from 8 keV to 15 MeV at the Dynamitron facility, Department of Nuclear Engineering of Tohoku University (FNL), and the quasi-monoenergetic neutron fields produced by $^{7}Li(p,n)$ reaction at four cyclotron facilities; Cyclotron and Radioisotope Center of Tohoku University (CYRIC), Institute for Nuclear Study of University of Tokyo (INS), Takasaki Research Establishment of Japan Atomic Energy Research Institute (JAERI) and Institute of Physical and Chemical Research (RIKEN).

## ESTABLISHMENT OF MONOENERGETIC AND QUASI-MONOENERGETIC NEUTRON CALIBRATION FIELDS

### *Dynamitron Neutron Field*

The monoenergetic neutron field was developed at the Dynamitron accelerator facility, FNL. Monoenergetic neutrons of 8 and 27 keV, 0.25 and 0.55 MeV, 1.0 and 2.0 MeV, 5 MeV, 15 MeV were

obtained in the forward direction to the incident beam axis by Sc(p,n), $^{7}$Li(p,n), T(p,n), D(d,n), T(d,n) reactions, respectively. The absolute neutron fluences were measured with $^{6}$LiF-SSD for 8 and 27 keV neutrons and with $^{235}$U fission chamber for other neutrons. The neutron fluence during the experiment was monitored simultaneously with the proton-recoil proportional counter. The neutron fluences were $1.0\times10^{2}$ n cm$^{-2}$ $\mu$C$^{-1}$ for 8 keV, $2.4\times10^{1}$ n cm$^{-2}$ $\mu$C$^{-1}$ for 24 keV, 1.0 - $4.0\times10^{4}$ n cm$^{-2}$ $\mu$C$^{-1}$ for others.

### *CYRIC Neutron Field*

The CYRIC neutron field has the 45 m long neutron TOF facility coupled with the beam chopping system and the beam swinger system. The quasi-monoenergetic neutrons of 22.0 and 32.5 MeV having 1.7 and 1.4 MeV FWHM were obtained from 2 mm thick $^{7}$Li target bombarded by 25 and 35 MeV protons, respectively, and the proton beam hit the target at 10 deg through the swinger magnet and was fully stopped at the Faraday cup. The neutrons were extracted in the TOF facility through the 50 cm thick iron-polyethylene collimator of 30 cm x 20 cm aperture settled in the 280 cm thick concrete wall of 100 cm x 50 cm aperture. The absolute neutron fluence of this field was measured with the proton recoil counter telescope (PRT) and the neutron spectrum was measured with the TOF method. The 22.0 and 32.5 MeV peak neutron fluences were $1.1\times10^{3}$ and $1.7\times10^{3}$ n cm$^{-2}$ $\mu$C$^{-1}$ at the collimator exit behind 8.6 m from the target. The neutron fluence during the experiment was monitored simultaneously with the $^{238}$U fission chamber fixed closely to the target.

### *INS Neutron Field*

The INS neutron field was used only for neutron irradiation and the irradiation samples were placed 10 cm away from the Li target in the forward direction, in order to get high neutron fluence and to depress the contribution of room-scattered neutrons, since the irradiation room is small in space. The neutron spectra are the same as those in the CYRIC neutron field. This field is now not available.

### *TIARA Neutron Field*

The TIARA neutron field was established in the neutron beam line collimated into 10 cm diameter. The 2 to 5 mm thick $^{7}$Li target settled in the cyclotron room was bombarded by the proton beam of 20 to 90 MeV at 0 deg and the protons passed through the target were bent down to the beam dump by a clearing magnet, and the neutrons produced at 0 deg were extracted through the 220 cm thick concrete wall. The absolute fluence of source neutrons was determined with PRT and the neutron fluence during the experiment was monitored simultaneously with the $^{238}$U and $^{232}$Th fission chambers fixed closely to the target. The FWHM of 40 and 65 MeV monoenergetic peak and the peak neutron yield have the respective values of 2.0 MeV and $2.1\times10^{4}$ n cm$^{-2}$ $\mu$C$^{-1}$, 2.1 MeV and $3.2\times10^{4}$ n cm$^{-2}\mu$C$^{-1}$, at the collimator exit behind 4 m from the target, for 43 and 67 MeV proton incidence. The neutron spectra measured with the TOF method.

### *RIKEN Neutron Field*

The RIKEN neutron field is now being established at the E4 experimental room of the separate sector ring cyclotron. The proton beam having energies of 80, 90, 100, 110, 120, 135, 150 and 210 MeV were injected on a 10 mm thick $^{7}$Li target through the beam swinger. Protons passed through the target were cleared out by the magnet and absorbed in the spectrograph. Neutrons produced at 0 deg were transported through the iron-concrete collimator of 20 cm by 20 cm aperture and 120 cm length. The neutron spectra were measured with the TOF method using BC501A and the absolute neutron fluence with the Li activation method using the $^{7}$Be activity from the $^{7}$Li(p,n)$^{7}$Be reaction.

## MATERIALS AND METHODS

### *Bi Spallation Detector*

Two sizes of natural bismuth samples were prepared. Thick samples are 80 mm diam by 10 mm thick and thin samples are 30 mm diam by 2 mm thick, which have chemical purities of 99.999 %.

The neutron reaction cross sections of Bi in the energy region from 20 to 210 MeV were measured by irradiating these samples in the p-Li quasi-monoenergetic neutron fields at INS, TIARA and RIKEN. The gamma-ray activities of the irradiated samples were counted by using a Ge detector and the reaction rates of identified radioisotopes were obtained after correction of self absorption and sum-coincidence effects.

By using the neutron energy spectrum $\Phi(E)$ and the reaction rate, A, the activation cross section $\sigma(E)$ can be estimated as follows. The reaction rate, A is divided into two parts; one is induced by the peak energy neutrons and the other by the low energy continuum neutrons, as

$$A = N \int_{Eth}^{Emin} \sigma(E)\,\Phi(E)\,dE + N\,\sigma(Ep)\,\Phi(Ep)$$

where N : number of target atoms relating to the relevant reaction,
$E_{th}$ : threshold energy,
$E_{min}$: lowest energy of monoenergetic peak neutrons,
$\sigma(Ep)$: cross section at peak neutron energy,
$\Phi(Ep)$: monoenergetic peak neutron flux.

If the threshold energy $E_{th}$ is higher than $E_{min}$, the first integration term must be zero. Otherwise, this term can be estimated by successive subtraction method using the neutron flux $\Phi(E)$ having lower peak energy. The $\sigma(E)$ values in lower energy region were cited from the evaluated data files, ENDF/B-VI (4), McLane et al. (5) and so on.

### *Organic Liquid Scintillation Detector*

The cylindrical organic liquid scintillator of 12.7 cm diam by 12.7 cm long NE-213 or BC501A is coupled to a R4144 photomultiplier connected to the E1458 base (Hamamatsu Photonics Co. Ltd.) which is specially designed to expand the dynamic range of output pulses for high energy neutron measurements. The detector size which stops the recoil proton up to about 120 MeV was selected in order to to be able to detect as higher energy neutrons as possible with keeping a good n-γ pulse-shape discrimination capability.

The response functions of the scintillator were measured at CYRIC, TIARA and RIKEN (6). At CYRIC, 35-MeV protons and 50- and 65-MeV $^3$He ions were injected into a 10 mm thick Be target. At TIARA, 67 MeV proton beam was injected into a 7.6 mm thick copper target, and at RIKEN, 135 MeV proton beam was injected into the Be (70 mm thick) + C (20 mm thick) target. These targets produced white spectral neutrons and the response functions down to a few MeV neutron energy were obtained by grouping them into monoenergetic interval with the TOF method coupled with the beam chopping system.

### *Si Semiconductor Dosimeter*

The dosimeter installs two neutron sensors and one gamma-ray sensor, which enables us to give neutron and gamma-ray doses at the same time (1,2). One type, slow neutron sensor, is an n-type silicon crystal on which a p+ layer of elementary boron enriched 94% $^{10}$B is deposited in about 1 mm thickness and the other type, fast neutron sensor, is an p-type silicon crystal without boron coating. Both crystals are contacted with 0.08 mm thick polyethylene radiators and in some cases only the slow neutron sensor is covered with thermal neutron filter of 0.5mm thick cadmium to improve its energy response. Figure 1 shows the schematic cross sectional view of two neutron sensors. The gamma-ray sensor is the p-type silicon detector of 3mm x 3mm without any radiator.

These three sensors are encapsulated in a metal package together with the charge sensitive preamplifier and the linear amplifier circuits. The output pulses from the sensors are counted through the pulse height discriminator and fed to the CPU for computing and displaying the dose equivalent values. The external size of the dosimeter is 100mm x 60mm x 20mm and its weight is about 170g.

The neutron detection efficiencies of these two sensors were measured in the monoenergetic neutron field at FNL. Monoenergetic neutrons of 0.2, 0.55, 1, 2, 5 and 15 MeV were produced using the Dynamitron accelerator. The dosimeter was placed in the forward direction to the beam axis. The efficiency measurement of the slow neutron sensor to thermal neutrons was done in the experimental hole of the TRIGA-II type reactor of Rikkyo University and in the thermal neutron field leaked from a graphite pile of the Institute of Radiation Measurements (IRM). The dosimeter was placed in front of a commercially available ellipsoidal water phantom, 45 cm high and 30 cm wide. The output pulses due to alpha particles produced by the $^{10}$B(n,α) reaction and protons recoiled from the elastic collision in the polyethylene radiator were measured with a multi-channel analyser, in this measurement.

### *CR39 Track Dosimeter*

The CR39 plastic has higher sensitivity than the NTA film for lower energy neutron, however many background etch-pits appear on the surface of nonirradiated CR39 plastic. In order to depress this background contamination, we diminished it by dyeing the CR39 plastic before etching with a KOH solution. The number of background etch-pits per cm$^2$ decreased about a factor of 10 after dyeing. As shown in Fig. 2, the CR39 dosimeter is contacted with two kinds of radiators, one is a 0.2 mm thick boron nitride for measuring low energy neutrons and the other is a 1 mm thick polyethylene for measuring fast neutrons.

The energy response of the CR39 etch-pits behind the two radiators were measured with the monoenergetic neutron field in the energy range of 8 keV to 15 MeV at FNL, graphite-moderated thermal neutrion fields at the Electro-Technical Laboratory and IRM, and the quasi-monoenergetic neutron field of 22 and 33 MeV at CYRIC. In these experiments, the dosimeter was also attached on a ellipsoidal water phantom.

## RESULTS AND DISCUSSIONS

### *Bi spalltion detector*

From the above experiments, we could identify the radionuclides of $^{207}$Bi to $^{196}$Bi produced by $^{209}$Bi(n,2n) to $^{209}$Bi(n,14n) reactions, respectively. Figure 3 indicates the cross section data of $^{209}$Bi(n,2n) to $^{209}$Bi(n,10n) reactions which have already been analyzed, in comparison with other experimental data (5) and the ENDF/B-VI high energy file data calculated by the ALICE code(4). Our data are generally in good agreement with them, but a large discrepancy can be found for Bi(n,9n) reaction, which might indicate a possibility of the inaccurate data of decay scheme and/or branching ratio of $^{201}$Bi . This figure clearly shows that the excitation functions of Bi(n,xn) reactions have simple and similar shapes, and the threhold energies differ at about 8MeV interval, which indicates that these reactions are quite useful for high energy neutron spectrometry.

The Bi detector has been used by our group to measure neutrons leaked through bulk shield of 3m thick iron and 1m thick concrete at ISIS of Rutherford Appleton Laboratory.

### *Organic Liquid Scintillator*

We obtained the neutron response functions of the scintillator by sampling neutron events into neutron energy intervals of 1, 2, 4, 5 MeV for neutron energy range from 0 to 44, 44 to 70, 70 to 90, 90 to 130 MeV, respectively (6). The response matrix of 68 neutron bin x 70 light output bin in the neutron energy range of 0 to 120 MeV was formed by using the measured response functions from 5 to 120 MeV neutrons and the SCINFUL Monte Carlo calculations (7) below 5 MeV neutron.

This detector has being used for neutron shielding experiment at TIARA and for thick-target yield experiment with heavy ions at the heavy ion medical synchrotron facility, National Institute of Radiological Sciences (HIMAC).

Figure 4 shows the cross-sectional view of the shielding experiment at TIARA. Inside the 340-cm-thick concrete shielding wall between the cyclotron room and the experimental room, an empty space of 120 cm x 120 cm x120 cm is equipped for shielding experiments. The concrete shield of 25 to 200 cm thickness and the iron shield of 10 to 130 cm thickness were fixed in contact with the 10.9-cm-diam collimator exit located at 4 m from the neutron target. The neutron energy spectra transmitted through shields were measured with the BC501A scintillator, using 40 and 65 MeV quasi-monoenergetic neutron sources which were produced by 43 and 68 MeV p-$^{7}$Li reactions. In Fig. 5, neutron spectra penetrated through concrete which were unfolded from the measured light output distributions with the FERDOU code (8) are compared with the MORSE Monte Carlo calculation (9) using the DLC-119/HILO86 group cross section library (10), as examples. This figure revealed in general the good agreement between experiment and calculation.

Figure 6 shows the schematic diagram of the experiment at HIMAC. Neutrons produced from a target bombarded by heavy ion beams were measured with three sets of the 12.7 cm diam by 12. 7cm long NE213 scintillators by the TOF method. A veto counter of 5 mm thick NE102A plastic scintillator was set in front of the NE213 to discriminate the secondary charged particles. A 0.5 mm thick NE102A scintillator fixed upstream to the target was used to produce beam pick-up signals for the TOF starting. The neutron energy spectra produced at 0 degree from 20 mm thick C, Al, and 10 mm thick Cu, Pb targets which were bombarded by 100 MeV/nucleon $^{12}$C ions are shown in Fig. 7, as examples.

### *Si Semiconductor Dosimeter*

Figure 8 shows the neutron detection efficiency of the dosimeter as a function of neutron energy. The measured results are the sum of the integrated counts given by the slow neutron sensor and the integrated counts of the fast neutron sensor multiplied by a factor of 20, in order to get the detection efficiency as close as possible to the fluence-to-dose-equivalent conversion factor given by ICRP-51 (11) which is drawn in a dotted line. In Fig. 8, the results calculated with the Monte Carlo method are also shown to compare with the measured results. Very Good agreement between experiment and calculation can be seen in the energy below 5MeV. Above 5MeV, the calculation underestimates the measured results due to the neglection of the contribution of charged particles which are produced in the silicon crystal itself and the surrounding material by various neutron reactions.

This dosimeter which combines two silicon sensors has neutron sensitivity over a wide energy range from thermal to 15 MeV and also has good energy response, excluding a large deviation from the ICRP-51 response curve in the energy range from 50 keV to 1 MeV, as seen in Fig. 8. Considering the energy response of the dosimeter shown in Fig. 8, the neutron dose equivalent H can be given by adding the neutron dose equivalent of energy higher than 1 MeV, $H_f$ and that of energy lower than 1 MeV, $H_S$. $H_f$ and $H_S$ are given by

$$H_f = K_f C_f \qquad \text{for En} \geq 1 \text{ MeV},$$
$$H_S = K_S C_S \qquad \text{for En} \leq 1 \text{ MeV},$$

where $C_f$, $C_S$ are the respective counts measured with fast sensor and slow sensor, $K_f$, $K_S$ are the respective conversion factor in units of μSv/count. The $K_f$ and $K_S$ values were determined as 0.5 and 10 μSv/count, respectively, from the estimation in the fission and 1/E slowing-down spectral fields.

In order to investigate the accuracy of this dose estimation method in a wide variety of actual neutron fields, we have done the field test of the dosimeter calibration in the following typical neutron fields having known neutron energy spectra; 1) moderated $^{252}Cf$ neutron source calibration field, 2) a beam extraction hole of the fast neutron source reactor of University of Tokyo, 3) labyrinth from the 40 MeV cyclotron room of Tohoku University, 4) MOX (Mixed Oxide) fuel handling room of Power Reactor and Nuclear Fuel Development Corporation, 5) 14MeV d-T neutron field penetrated through concrete shield, and 6) On the outer surface of the concrete shield surrounding several hundreds MeV electron synchrotron. In these field tests, the dosimeter was fixed on the water phantom faced to the neutron beam direction. The measured counts were compared with the dose equivalent values obtained from the dose equivalent counters (rem counters) of Studsvik Co. 2202D and Fuji Electric Co. NSN1 which were used as neutron dose monitors.

Figure 9 summarizes the results of these field tests. The ratio of neutron dose equivalent value measured with this personal dosimeter to that with the rem counter is shown as a function of neutron energy in the test field averaged by weighting with the dose equivalent. The ratio must be equal to 1 for the ideal dosimeter, and our personal dosimeter gives neutron dose equivalent within a factor of 2 margin of accuracy, excluding a special field in which thermal neutron fluence occupies more than 50% of total neutron fluence, such as at some positions in the labyrinth from the cyclotron room. Even in such a field, we can estimate the neutron dose equivalent within a factor of 3 by using a thermal neutron sensor with Cd cover and moreover with much better accuracy by adjusting the conversion factor $K_S$ slightly.

### *CR39 Track Dosimeter*

Figure 10 shows the weighted sum of the energy response of the dosimeter with two radiators, boron nitride (BN) and polyethylene (poly), in order to give a best fit to the ICRP51 response curve. The data at thermal, and 8 keV up to 15 MeV energies are the measured results (shown in white circles and triangles), and the data between thermal and 8 keV energies are the calculated results with the Monte Carlo method (in white squares). Good agreement between experiment and calculation can be seen and the energy response of this dosimeter well fits the ICRP51 response curve in the energy range lower than about 10 MeV. In order to improve the energy response above 10 MeV, the weighting factor was further increased only for the etch-pits having a diameter larger than 20 μm, considering that the diameter of etch-pits increases with neutron energy. The thus-adjusted energy response of the dosimeter is also shown as white square signs in Fig. 10 and indicates much better agreement with the ICRP51 response curve above 10 MeV. The dose equivalent in mSv is then given by the following formula,

$$H\,(\text{mSv}) = \{\text{BN}/8 + [\text{poly1} + (\text{poly2} - 100) \times 8] \times 8\ \} \times 10^{-4}$$

where BN, poly1 and poly2 are the etch-pits per $cm^2$ of CR39 with BN and those having a diameter smaller and larger than 20 μm with polyethylene radiators, respectively. If poly2 is less than 100, the third term of the above formula is neglected.

## CONCLUSION

We have developed two types of high energy neutron spectrometers, and active and passive personal neutron dosimeters. The two spectrometers are now in use for neutron spectrometry at accelerator facilities and these two dosimeters will be commercially available very soon.


## ACKNOWLEDGMENTS

The authors wish to thank Dr. Y. Kumamoto and Mr. A. Fukumura for their kindful cooperation during the HIMAC experiment and the machine group members for their four cyclotron operations during our experiments.

## REFERENCES


1. T. Nakamura, N. Tsujimura, T. Yamano, T. Suzuki, and E. Okamoto, J. At. Energy Soc. Japan, 36 337-345 (1994), in Japanese.
2. T. Nakamura, N. Tsujimura, and T. Yamano, Appl. Radiat. Isot., 46, 469-470 (1995).
3. H. Ohguchi, T. Nakamura, M. Baba, M. Takada, and N. Nakao, Appl. Radiat. Isot., 46, 509-510 (1995).
4. National Nuclear Data Center, Brookhaven National Laboratory, "Evaluated Nuclear Data File", ENDF/B-VI (1990).
5. V. McLane, C.L. Dunford and P.F. Rose, "Neutron Cross Sections", Vol.2, Neutron Cross Section Curves, Academic Press Inc., New York (1988).
6. N. Nakao, T. Nakamura, M. Baba, et al., Nucl. Instrum. Methods, A362, 454-465 (1995).
7. J. K. Dickens, ORNL-6463, Oak Ridge National Laboratory (1988).
8. K. Shin, Y. Uwamino, and T. Hyodo, Nucl. Technol., 53, 78 (1981).
9. G. R. Straker, P. N. Stevens, D. C. Irving, and V. R. Cain, ORNL-4585, Oak Ridge National Laboratory (1970).
10. R. G. Alsmiller Jr., J. M. Barnes, and J. D. Drischler, ORNL/TM-9801, Oak Ridge National Laboraotyr (1986).
11. ICRP Publ. 51, Ann. ICRP, 17 (1987).


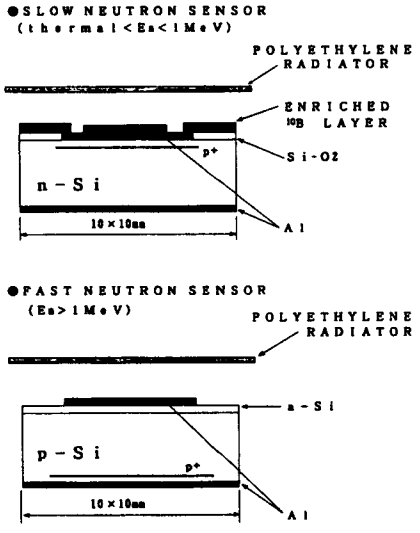


Fig. 1 Schematic cross sectional view of two silicon neutron sensors

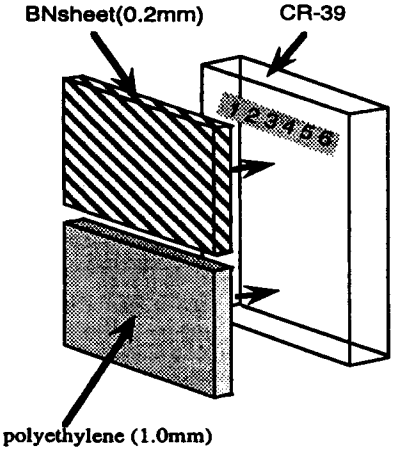


Fig. 2 Schematic view of CR39 plastic with two radiators

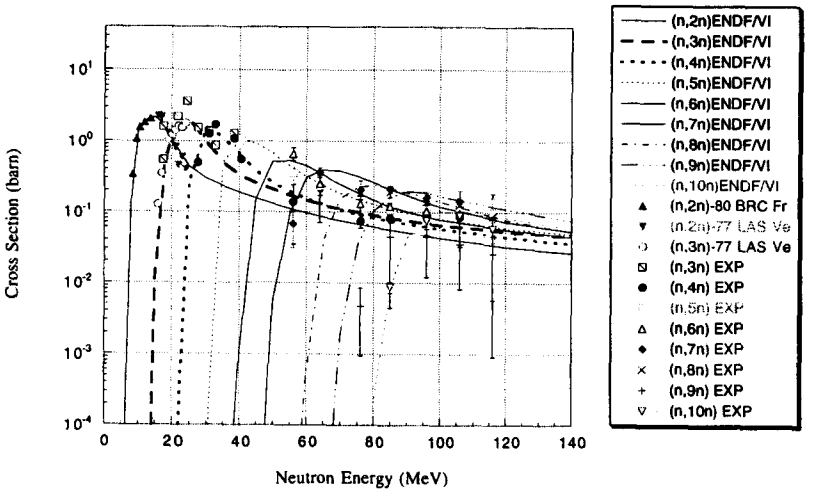


Fig. 3 Measured cross section data of $^{209}Bi(n,xn)$ reactions compared with ENDF/B-VI (4) and other experimantal Data (5)

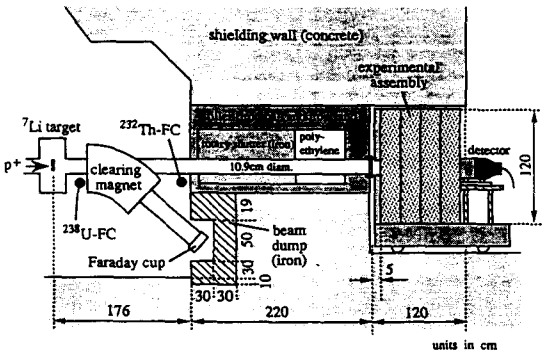


Fig. 4 Cross sectional view of the shielding experiment at TIARA

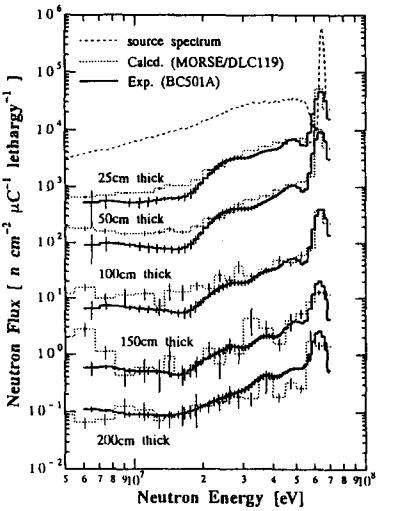


Fig. 5 Comparison of neutron spectra transmitted through concrete of various thicknesses between experiment and MORSE calculation for 65 MeV quasi-monoenergetic neutron source

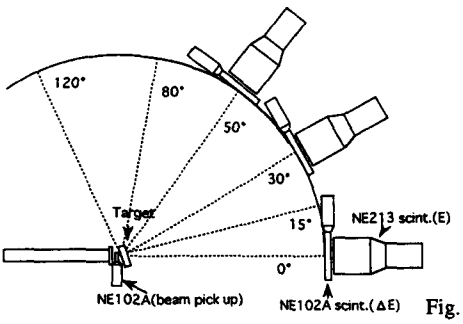


Fig. 6 Schematic diagram of the thick-target yield experiment at HIMAC

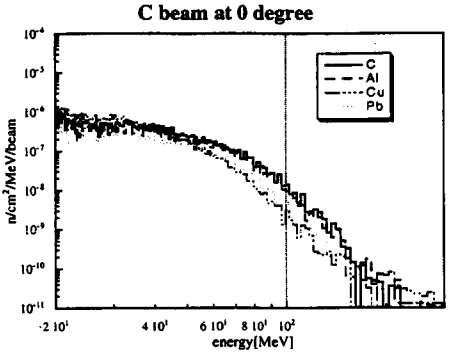


Fig. 7 Neutron spectra produced at 0 degree from 20-mm thick C, Al and 10-mm thick Cu, Pb targets bombarded by 100 MeV/nucleon C ions

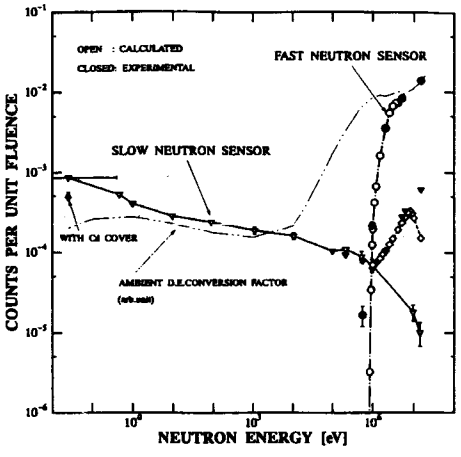


Fig. 8 Comparison of measured and calculated neutron detection efficiencies of the Si dosimeter, together with the ICRP-51 fluence-to-dose-equivalent conversion factor

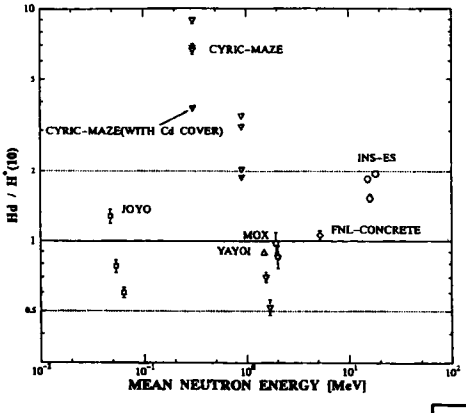


Fig. 9 Comparison of dose equivalent given by the Si dosimeter to that by the rem counter for various neutron fields having different mean neutron energies

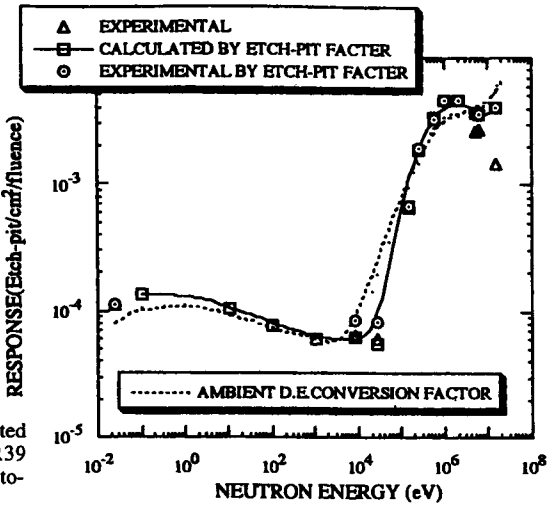


Fig.10 Comparison of measured and calculated neutron detection efficiencies of the CR39 dosimeter, together with the ICRP-51 fluence-to-dose-equivalent conversion factor